Molecular Physics
Vol. 107, No. 2, 20 January 2009, 171–179

Taylor & Francis
Taylor & Francis Group

RESEARCH ARTICLE

The molecular basis for the behaviour of niobia species in oxidation reaction probed by theoretical calculations and experimental techniques

Teodorico C. Ramalho[a]*, Luiz C. A. Oliveira[a], Kele T. G. Carvalho[a], Eugênio F. Souza[a], Elaine F. F. da Cunha[a] and Marcelo Nazzaro[b]

[a]*Universidade Federal de Lavras, Depto. Química, Caixa Postal, CEP 37200-000, Lavras-MG, Brasil;* [b]*Laboratorio de Ciencias de Superficies y Medios Porosos, Depto de Física, UNSL, 5700 San Luis, Argentina*

(*Received 26 November 2008; final version received 21 January 2009*)

This paper describes the preparation and use of a new class of materials based on synthetic niobia as catalysts in the oxidation of organic compounds in aqueous medium. The chemical reactions were carried out in the presence of hydrogen peroxide (H_2O_2). The material was characterized with X-ray diffraction, XPS and H_2-TPR (temperature-programmed reduction) measurements. The organic molecule methylene-blue was used in the decomposition study as a probe contaminant. The analysis using the ESI-MS technique showed complete oxidation observed through different intermediates. This suggests the use of niobia species as an efficient Fenton-like catalyst in degradation reactions. Theoretical quantum DFT calculations were carried out in order to understand the degradation mechanism.

Keywords: niobia; Fenton-like mechanism; DFT calculations; ESI-MS

1. Introduction

It has been reported that niobium is interesting and important for some catalytic reactions, and therefore the research and development of niobium compounds in catalytic applications have increased in recent years [1]. However, reports on the use of pure niobium oxides as a catalyst for the oxidation of contaminants in aqueous medium are scarce. A study has been reported with niobium oxides as a catalyst for hydroxylation, but combined with an inorganic cation at high temperature [2]. In general, research focuses on the study of the catalytic performance of Nb_2O_5 impregnated with metal oxides [3]. The particular properties of niobium, such as, redox properties, photosensitivity, acidity and catalytic behaviour [4], constitute the motivation to understand and use niobium for catalytic purposes. Some important materials have been used as catalyst supports or promoters, but we are interested in the utilization of niobia. The natural abundance of niobium in the Earth's crust is about 20 ppm in mass. Distributed by country, Brazil is the main niobium-supplier, providing about 60% of the world production. In spite of the increasing interest in applications of niobium compounds in many technological fields, the niobium chemistry is not as deeply dominated as other more common industrial metals used in heterogeneous catalysis [5]. Niobium-based materials are effective catalysts in numerous reactions, such as pollution control, selective oxidation, hydrogenation and dehydrogenation, photochemistry, electrochemistry and polymerization. A remarkable application of niobium-based compounds is in oxidation catalysis such as the Fenton reaction. The Fenton reaction involving hydrogen peroxide and a ferrous catalyst is currently one of the most powerful oxidizing reactions available [6].

The main purpose of this work was to prepare a new class of materials based on a natural niobium oxide (niobia) to act as a catalyst for textile dye oxidation through a Fenton-like mechanism. In addition, some experiments have been carried out to study the effects of natural and synthetic Nb_2O_5 on the degradation of organic dye in the presence of hydrogen peroxide. The reaction mechanism of the heterogeneous dye/niobia/H_2O_2 system has been studied on-line by ESI-MS and theoretical calculations.

2. Methodology

2.1. *Materials and characterization*

In this work two different materials were utilized for the oxidation reaction in the presence of H_2O_2: (i) a synthetic niobia prepared in our laboratory (synthetic niobia) and (ii) this synthetic niobia previously

*Corresponding author. Email: teo@ufla.br

ISSN 0026–8976 print/ISSN 1362–3028 online

DOI: 10.1080/00268970902769489
http://www.informaworld.com

treated with H_2O_2 (30% v/v), called synthetic niobia//H_2O_2. Synthetic niobia was prepared from $NH_4[NbO(C_2O_4)_2(H_2O)](H_2O)_n$ (supplied by CBMM-Companhia Brasileira de Metalurgia e Mineração, Araxá-MG) and NaOH (50 mL, 1 mol L^{-1}) by co-precipitation followed by thermal treatment at 60°C (72 h) [7].

The powder XRD data were obtained in a Rigaku model Geigerflex using Cu Kα radiation scanning from 2 to 75° at a scan rate of 4° min^{-1}. XPS data were obtained by KRATOS Analytical XSAM 800 cpi ESCA equipped with a Mg anode (Mg Kα radiation, 1253.6 eV) and spherical analyzer operating at 15 kV and 15 mA. H_2-TPR (temperature-programmed reduction) profiles were obtained in Chembet 3000 Quantachrome equipment.

2.2. *Catalytic studies*

Experimental degradation tests were carried out at 25°C using methylene blue dye (50 mg/L) and niobia catalyst (10 mg) in an oxidant solution comprised of H_2O_2 (97 mmol). The oxidant solution was stirred for 2 min prior to mixing with the dye and the niobia. The reactions were monitored by UV–vis measurements (Shimadzu-UV-1601 PC). All the reactions were carried out under magnetic stirring in a recirculating temperature controlled bath kept at 25 ± 1°C.

2.3. *Studies by ESI-MS*

In an attempt to identify the intermediate formation, the methylene blue decomposition was also monitored with the positive ion mode ESI-MS of an Agilent MS-ion trap mass spectrometer. The reaction samples were analyzed by introducing aliquots into the ESI source with a syringe pump at a flow rate of 5 mL min^{-1}. The spectra were obtained as an average of 50 scans of 0.2 s. Typical ESI conditions were as follows: heated capillary temperature 1508°C; sheath gas (N_2) at a flow rate of 20 units (*ca* 4 L min^{-1}); spray voltage 4 kV; capillary voltage 25 V; tube lens offset voltage 25 V.

2.4. *Computational methods*

The calculations were carried out with the *Gaussian98* package [8]. All the transition states, intermediates and precursors involved were calculated. Each conformer was fully optimized by DFT. The energy profile at selected DFT geometries along the reaction pathway was computed at B3LYP level of theory using the 6-31+G(d, p) basis set. This computational procedure has been employed previously on similar systems with success [9,10]. Furthermore, after each optimization the nature of each stationary point was established by calculating and diagonalizing the Hessian matrix (force constant matrix). The unique imaginary frequency associated with the transition vector (TV) [7,9], i.e. the eigenvector associated with the unique negative eigenvalue of the force constant matrix, was characterized. The solvent effect was evaluated with the utilization of polarized continuum model (PCM) solvation calculations, initially proposed by Tomasi and Barone [11,12]. The final structures were submitted to analysis of natural bound order (NBO) [13,14] with the density functional Becke's three-parameter exchange functional and the gradient-corrected functional of Lee, Yang, and Par (B3LYP) using the basis set 6-311G** [15]. All the minima connected by a given transition state were confirmed by intrinsic reaction coordinate (IRC) driving calculations [16,17] (in mass-weighted coordinates) as implemented in *the Gaussian98* program [8]. Electronic transition energies were computed by CISD calculation at the Hartree-Fock level employing basis 6-31G. All UV calculations were also carried out using *Gaussian98* [8].

For all the studied species we have checked S2 values to evaluate whether spin contamination can influence the quality of the results. In all cases we have found that the calculated values differ from $S(S+1)$ by less than 10%.

3. Results and discussion

3.1. *Characterization*

XRD patterns for the samples indicate that the niobias are amorphous. These results are in very good agreement with other experimental studies [18].

The samples were characterized using XPS techniques, the spectra are reported in Figure 1. The XPS Nb3d5/2 spectra of the pure niobia and niobia treated with hydrogen peroxide (Figure 1) are very similar and show the same peaks from Nb_2O_5 reported in the literature. This means that the treatment with H_2O_2 does not change the structure of the niobium species significantly. There are two well defined peaks at 207.1 and 209.8 eV that correspond to the reported binding energies of Nb_2O_5. The formation of hydroxyl groups on the niobia surface was identified by the XPS O1s spectrum and reported by Oliveira *et al*. [18,19].

In Figure 2, the reduction profile for synthetic niobia and this sample previously treated with H_2O_2 is observed. The synthetic niobia was reduced starting at 415°C, suggesting the reduction of NbOx superficial species. The intense reduction step occurs at 800°C and refers to the reduction of bulk of the niobia.

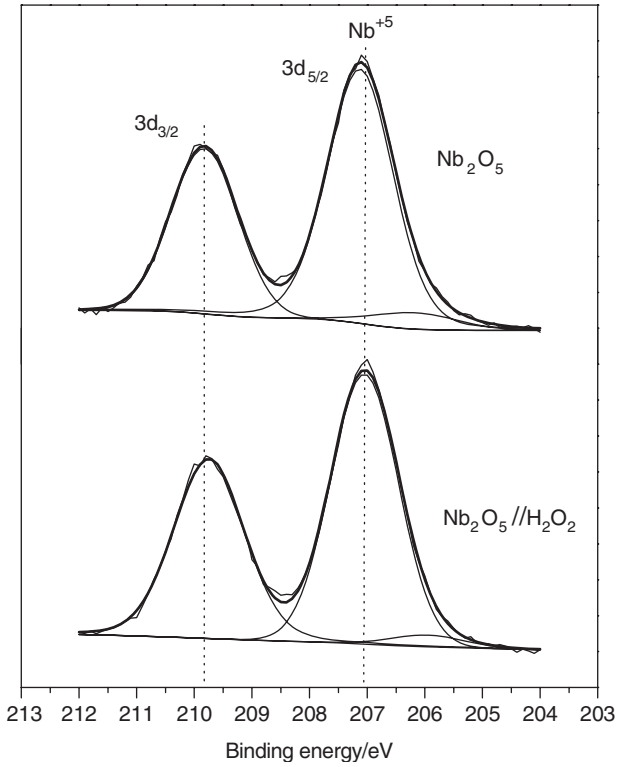

Figure 1. XPS profiles of Nb 3d region of niobias.

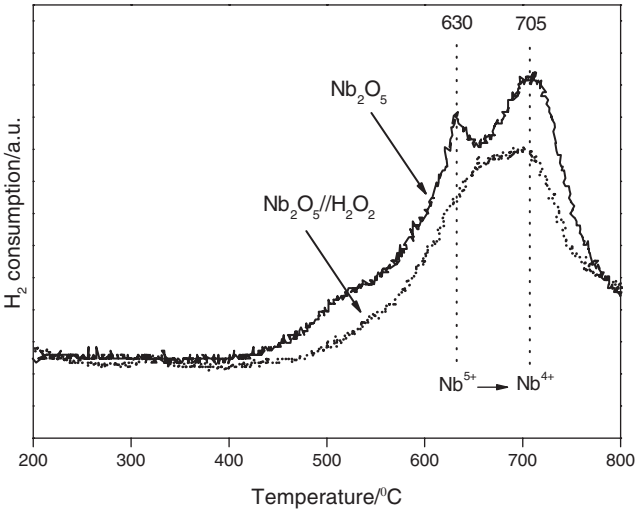

Figure 2. FTIR spectra for pure and H_2O_2-treated niobias.

The partial reduction of the support could also be confirmed through the change of the sample color from white to gray after TPR analysis [20]. It is interesting to observe that a decrease of superficial niobia occurs in the niobia after treatment with H_2O_2 (niobia//H_2O_2) suggesting that the hydrogen peroxide could act as a reducing agent, which promotes the formation of reduced niobium phases on the surface.

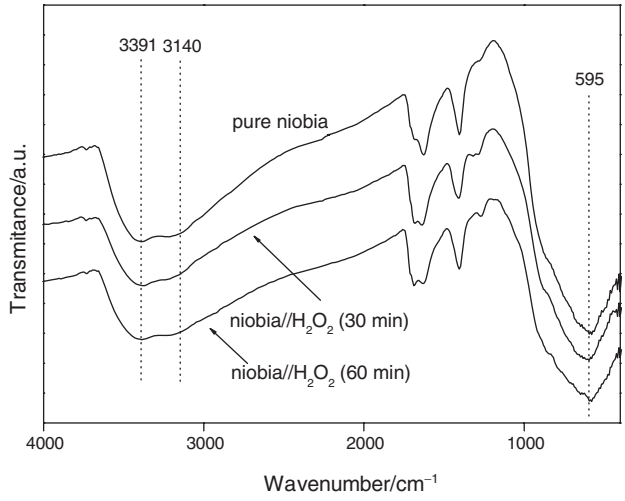

Figure 3. H_2–TPR profiles for pure and H_2O_2-treated niobia.

The presence of hydroxyl groups was also confirmed by FTIR spectroscopy (Figure 3). Both samples showed a broad band centered at 595 cm^{-1} and a shoulder at 895 cm^{-1}, which can be attributed to the amorphous niobia. The band at 1629 cm^{-1} for the pure niobia is due to the bending vibrations of the H_2O molecules. The broad band at 3391 cm^{-1} can be attributed to the OH-stretching vibration of H_2O molecules and a typical signal at 3140 cm^{-1}, due to the bulk hydroxyl stretching [18]. Intensity of this band had increased confirming increased quantity of superficial hydroxyl (3391 cm^{-1}) after H_2O_2 pre-treatment.

3.2. *Catalytic studies*

The oxidation of the textile dye methylene blue with H_2O_2 in presence of the synthetic niobia and synthetic niobia//H_2O_2 was also studied. The identification of reaction intermediates was performed on-line by the ESI-MS equipment during the oxidation of the methylene blue dye after 60 min of reaction (Figure 4). After 60 min of reaction time, strong signals corresponding to $m/z = 300$; 316, 347 and 384 were detected, due to successive hydroxylation of the dye structure. The previous treatment of the niobia with H_2O_2 leads to much higher catalytic activity for the synthetic niobia. Actually, from Figure 4, the increasing number of reaction intermediates can clearly be observed after the same reaction time and also the complete disappearance of the signal $m/z = 284$.

3.3. *Reaction mechanism: substrate point of view*

The intermediate structures are reported in Figure 5. The calculation of the Gibbs free energy for the

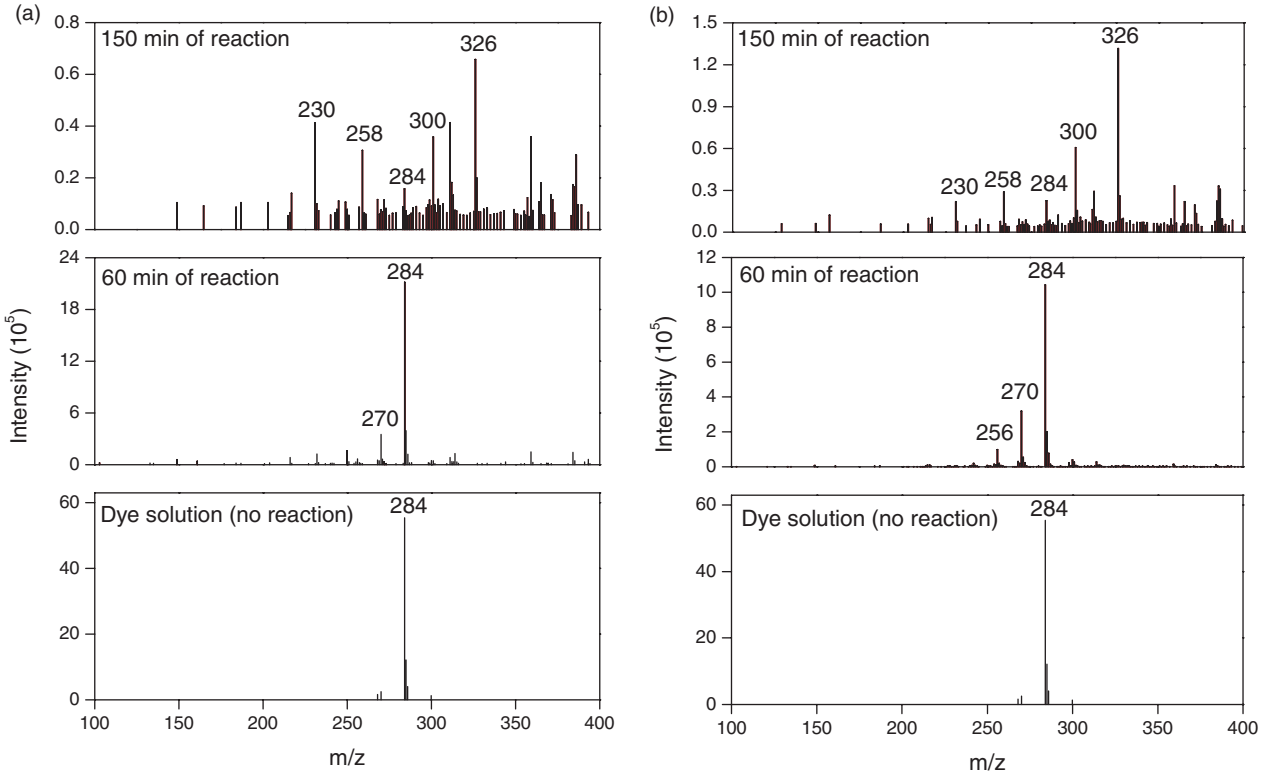

Figure 4. ESI mass spectra in the positive ion mode for monitoring the oxidation of methylene blue dye in water by the pure niobia (a) and niobia treated with hydrogen peroxide for 60 min (b) via photocatalysis at different reaction times.

stability of the intermediates was performed by the method implemented in the *Gaussian98* package [8]. The resulting energy values are shown in Table 1. The intense signal corresponding to $m/z = 300$ (Figure 4) result from the hydroxylation in the aromatic ring. According to data listed in Table 1, it can be observed that the hydroxyl group at the C2 position is about +3.30, +6.04, +7.86 and +8.68 kcal mol^{-1} more stable than the alternative C3, C5, N and S, respectively.

In order to get a deeper insight on the peak m/z 300, we calculated at DFT level, the Gibbs free energy for the stability of some possible isomers with m/z 300. From our data, we can see that in the most stable fragment, the hydroxyl group is at C2 position. This certainly corroborates our previous findings [18,19] and reinforces the earlier reaction mechanism proposed, which involves the generation of hydroquinone or hydroquinone-like intermediate and the redox cycle of hydroquinone/quinone in the Fenton reaction. That is an unstable key-intermediate that points out the high probability of a quick rupture of both chemical bonds C1–C2 and C5–C6 (Figure 5).

Further calculations revealed that the hydroxylation occurs at C4, which explains the resulting intense signal corresponding to $m/z = 316$. Thus, the compounds **II** and **III** (Figure 5) are supposed to be stable and the reaction path may still involve other hydroxylations. From these results, the third hydroxylation would more likely occur at 5′ position. This is a critical step, as it would simultaneously lead to the formation of hydroquinone or hydroquinone-like intermediates generated by the *OH attack. This is an unstable key-intermediate, as mentioned above. This could justify the formation of **V** ($m/z = 130$). Due to the presence of *OH in the reaction medium, the oxidation of **V** probably occurs, which consequently generates the stable specie **VI**, with $m/z = 160$. These calculations show good agreement with the experimental data (Figure 4). Surprisingly, the fragmentation pathway is quite similar to the one described in our previous study [19]. This could strongly suggest that the reaction with niobia catalyst is started by the activation of H_2O_2 to produce an *OH radical.

3.4. *Reaction mechanism: catalyst point of view*

In order to investigate the best model to describe the so called synthetic niobia//H_2O_2, we have used the hexa-cluster (C–I_{hexa} – interaction between catalyst

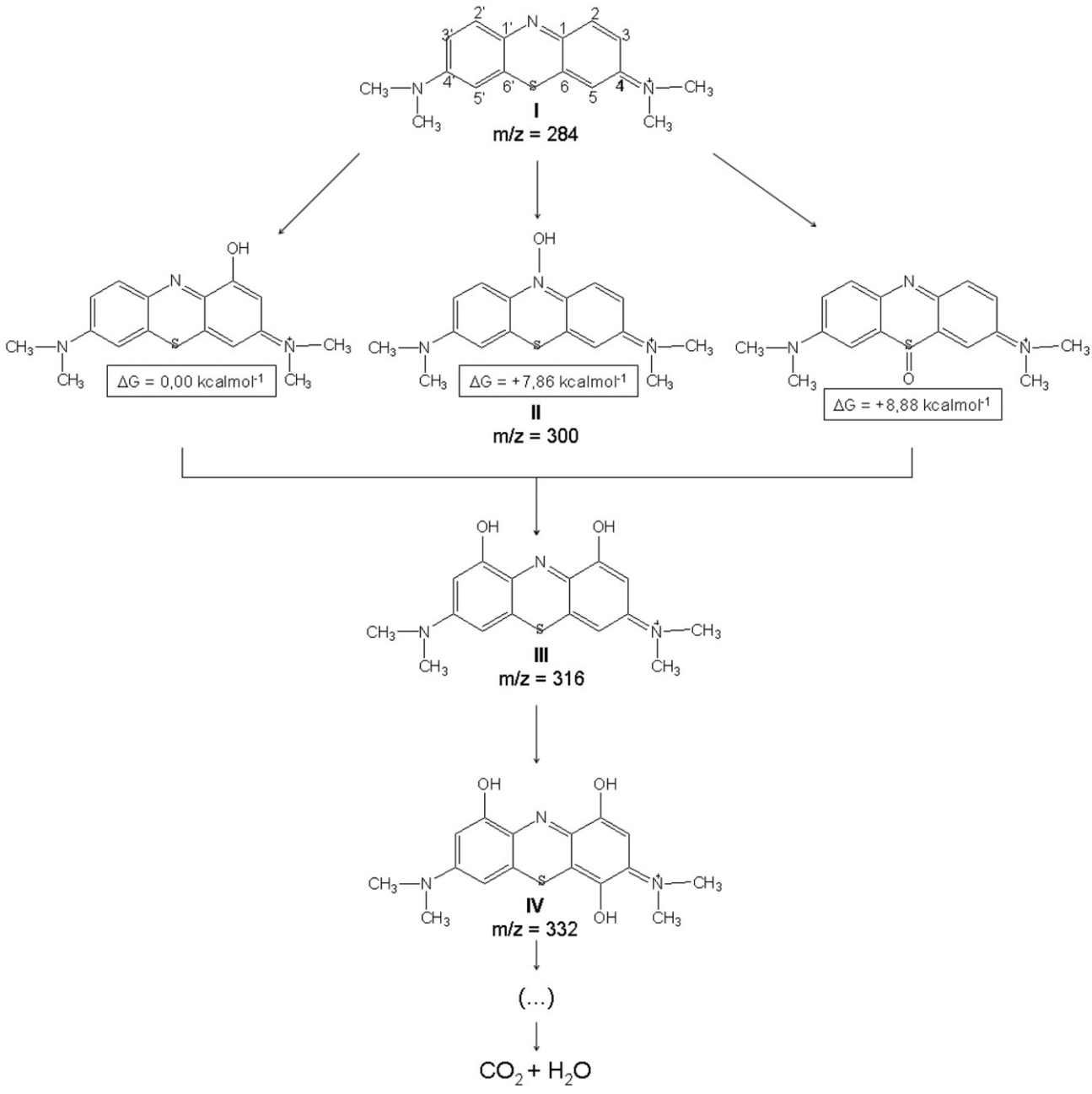

Figure 5. Scheme with intermediates proposed for the oxidation of methylene blue dye ($m/z = 284$).

and peroxide molecule through hydrogen bond) and octa-cluster (peroxo-complex C–I_p). A similar cluster hexa-cluster or octa-cluster was used in previous studies to model the niobia framework. According to our calculation, C–I_{hexa} has a higher energy barrier for its formation than octa-cluster (peroxo-complex C–I_p), about $+32.52\,kcal\,mol^{-1}$. This means that the peroxo-complex C–I_p is the more stable structure to describe the formation of the synthetic niobia//H_2O_2. We are quite aware of the limitations of this cluster-model, but as shown in other publications, at least for small sized substrates, the larger clusters do not introduce any changes in the mechanism, but only in the energetics of the reactions [16]. Therefore, the mechanism of the reaction, as well as the relative energies, can be well established with that model.

In order to check the peroxo-complex model to understand the overall reaction mechanism, molecular orbital calculations were performed by the algorithm implemented in the *Gaussian98* package [8] with the

CIS technique [22]. This method is a powerful tool for the computation of UV parameters. These peroxo species are potential oxygen donors to organic substrates in the liquid phase. The niobium and peroxo niobium complexes exhibit absorption bands at 263.1 and 298.5 nm, respectively.

From our theoretical data, a strong band at 253.1 nm for niobium complex is red-shifted as compared to the peroxo niobium complex, which generates a decrease in the band gap from 4.71 to 4.15 eV. This is in good agreement with the experimental results from DRIFTS-UV [21] and it could, in principle, justify the formation of the niobia previously treated with H_2O_2 (pure niobia//H_2O_2) [18]. The direct coordination of Nb with peroxide molecule to favor the formation of the peroxo-complex is then possible (Figure 6).

Table 1. Gibbs free energy of II and III intermediates using B3LYP/6-31+G(d, p).

Intermediate	Hydroxyl position	ΔG (kcal mol^{-1})
II	2	0.00
	3	+3.30
	N	+7.86
	S	+8.68
	5	+6.65
III	2, 2′	0.00
	2, 5′	+34.69
	3, 2′	+11.73
	3, 3′	+14.26
	3, 5′	+3.25
	5, 5′	+21.22

In a theoretical calculation of the type reported here, there is a primary consideration: the choice of the basis set and the form of the exchange-correlation functional. For carbon and oxygen, we have used a large all electron 6-311++G** [23] basis set, and, for niobium, we have used a pseudopotential and an associated basis set [24]. From our calculation, good agreement between the calculated and experimental geometry for niobium complex [25] was observed. After the optimization of the selected conformers, a force constant calculation was carried out to assure that the conformers reported are all local minima and that the structures reported in Tables 1 and 2 are intermediates [26].

We have employed theoretical calculations to obtain the relative chemical stability of the complexe's intermediates (**C–I$_p$**) with Nb charges of +3, +4 and +5, the low energy associated to the intermediates was attributed, for instance, to the forming of strong n_{Nb}/σ^*_{O-O}, n_{Nb}/σ^*_{O-H}, $\sigma_{O-H}/\sigma^*_{O-O}$ $\sigma_{O-O}/\sigma^*_{O-H}$ and $\sigma_{Nb-O}/\sigma^*_{O-H}$ interactions (Table 3).

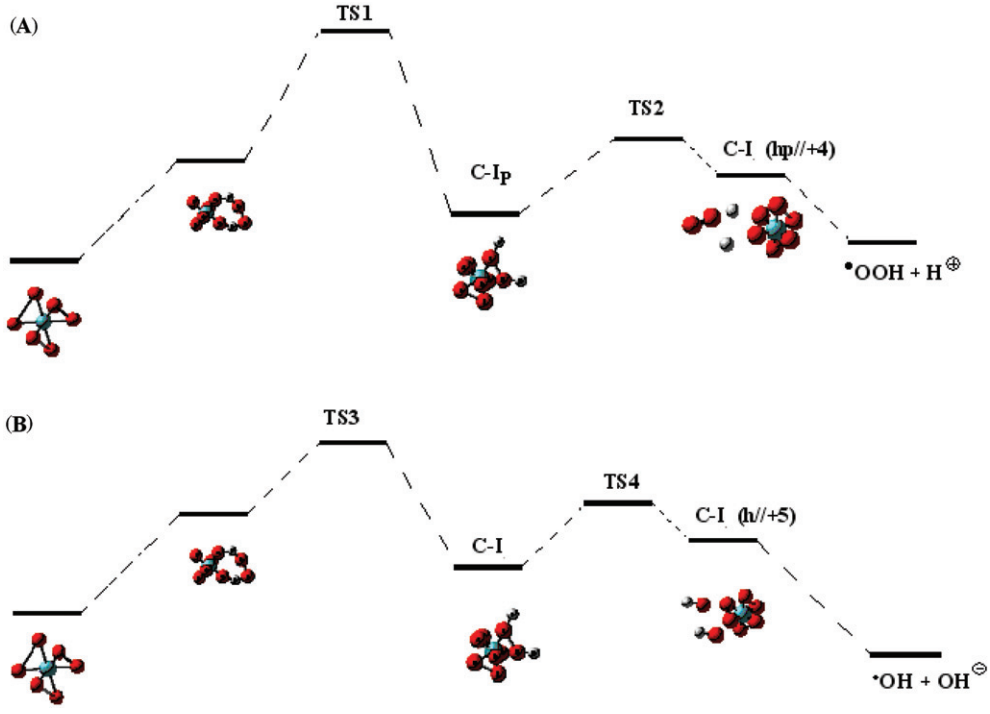

Figure 6. Model structures for the catalyst.

Non-bonded interactions play an important role in the complex stabilization [27]. For instance, studies with 69 aditional published crystal structures of organic, inorganic, and organometallic compounds containing divalent sulfur (S bonded to two ligands, Y and Z, different from H) revealed that, in the lattice, electrophiles tend to approach the sulfur atom roughly 20° from a line perpendicular to the Y–S–Z atoms plane, whereas nucleophiles tend to approach approximately along the extension of one of the sulfur covalent bonds [28,29]. We believe that these regularities portray features of the electron distribution and indicate the preferred direction of approximation of electrophiles and nucleophiles, as well as the preferred direction for nonbonded interactions. These features are not observed with the same intensity in the case of niobium [30]. The generated peroxo-complex **C–I$_p$** has two possible reaction pathways. The first one, is the formation of the **C–I$_p$(hp)** (**C–I$_p$(hp)** $\rightarrow$ $^{\bullet}OOH + H^+$) and the second one is the formation **C–I$_p$(p)** (**C–I$_p$(p)** $\rightarrow$ $^{\bullet}OH + OH^-$). From our calculations, it is clear that **C–I$_p$(h)** is less stable than **C–I$_p$(hp)** about 10.2 kcal mol^{-1}. Several papers describe powder X-ray diffraction of Nb and Ta peroxo complexes [31–34]. Thus the peroxo-complex of niobium probably occurs in solution and our previous experimental findings are in line with this conclusion also [18,19]. Therefore, the reaction mechanism, as well as the relative energies, can be well established with the peroxo-complex model. This theoretical consideration is in good agreement with experimental results from other groups [35,36].

In order to investigate the oxidation state of the niobium atom in the peroxo-complex, we performed theoretical calculations on the reaction pathway of the hydroperoxo complex (**C–I$_p$(hp)**) in three possible niobium oxidation states [37]. Thus to get more insight, the electrostatic charges were determined so as to reproduce the B3LYP/6-311++G** quantum molecular mechanical electrostatic potential (MEP) [38]. This means that it was necessary to produce charges that fit into the electrostatic potential at points selected according to the CHelpG scheme [39,40]. As expected, the most favorable niobium states of oxidation are either +5 or 3+ in the initial complex which is consistent with the literature [37]. Furthermore, it is well known that Nb atom in niobia is limited almost entirely to the +5 state of oxidation. However, it is an interesting fact that niobium could develop to +4 charge in the peroxo-complex, in other words **C–I$_p$(+4)** is the most stable complex. This behaviour remains in the other transformation steps of reaction, for instance, at the rupture of the O–H chemical bond (Figure 5), the most favourable complex formed is **C–I$_p$(hp//+4)**. Nevertheless when the rupture of the O–O chemical bond (Figure 5) occurs, **C–I$_p$(h//+5)** is formed. So, our theoretical findings suggest that the first step of the reaction is the formation of **C–I$_p$(hp)** and subsequently *OOH.

In addition, our results also point out the formation of reactive species, partially reduced niobia, on niobia surface with peroxide. These theoretical insights are in good agreement with experimental data from TPR analyses.

In the first step of transformation, the highest energy associated to the transition states was attributed to the formation of the peroxo-complex (TS1) (Table 4). The energy profile of the second step is very similar to step 1. However, a lower energy barrier is observed for the formation of the transition states

Table 2. Relative Gibbs free energy (kcal mol^{-1}) among the intermediates with the Nb charge +3, +4 and +5.

Nb Charge	Complex-hexa	C–I$_p$	C–I$_p$(hp)	C–I$_p$(h)
+3	+1.81	+40.36	+41.56	+31.0
+4	+20.65	0.00	0.00	+27.74
+5	0.00	+1.52	+35.53	0.00

Table 3. Orbital interaction energies (ΔE2, kcal mol^{-1}) for **C–I** compounds.

Charge system	n_{Nb}/σ^*_{O-O}	n_{Nb}/σ^*_{O-H}	$\sigma_{O-H}/\sigma^*_{O-O}$	$\sigma_{O-O}/\sigma^*_{O-H}$	$\sigma_{Nb-O}/\sigma^*_{O-H}$
+3	0.24	1.73	6.73	4.58	0.80
+4	0.10	1.93	6.71	4.58	8.24
+5	0.31	1.71	6.72	6.80	2.65

Table 4. Activation energy (kcal mol^{-1}) of the transition states.

Nb charge	TS1	TS2	TS3	TS4
+3	53.78	42.45	35.12	30.74
+4	44.54	26.47	18.63	23.41
+5	45.87	29.89	26.45	14.65

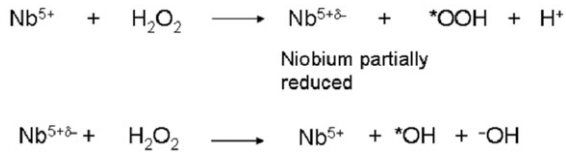

Figure 7. Proposed catalytic cycle.

(TS3 and TS4) when compared to TS1 and TS2. As argued previously, the positive charge is best stabilized through direct participation of the non-bonded oxygen electrons, the product formed being **C–I$_p$(hp)** with the energy of the transition state of + 44.54 kcal mol^{-1}. The energies of the transition states for the second step are lower than for the first step (see Table 1). It also was observed experimentally that the slowest step is the formation of the Nb^{+4} intermediate (step 1) [13,14]. Ongoing from Nb^{+5} to Nb^{+4}, there is a decrease in the energy barrier for the formation of the transition states, as shown in Table 4. Certainly, those transition states and intermediate energies modulate the reaction profile of niobia species for the oxidation reaction.

It must be remarked that density functional theory (DFT) with the B3LYP nonlocal exchange correlation functional has been applied as well to study these molecules. For each transition state localized at this level of theory, intrinsic reaction coordinate (IRC) calculations have been performed as well. Thus, the products and reagents connected by the respective transition states have been unambiguously localized.

Our results showed that the Nb_2O_5 is a potential catalyst for the hydrogen peroxide decomposition producing hydroxyl radical (*OH) by the Fenton-like system. In line with that observation, we can propose the scheme described in Figure 7 for the behaviour of niobia species as efficient Fenton-like catalyst. Comparison between theoretical and experimental data shows that many similarities exist. In both situations, indeed, the most likely reaction mechanism involves, as a first step, the formation of a stable complex whose formation is dominated by the donor–acceptor mechanism. The charge upon niobium (Table 2), after interaction, is partially reduced suggesting a trend of a contribution of peroxide → metal charge transfer, which agrees to the known surface acidity behavior and TPR analyses. Otherwise, Lewis acids will cause some change in the orbital occupancies. Therefore the occupancy of donor orbitals are of major interest. The Natural Bond Orbital (NBO) analysis of the occupancies of the **C–I$_p$** complex show that the most significant change upon interaction is the decrease of occupancy of the O–H chemical bond from 1.94 to 1.62.

Thus, to determine the relative chemical stability of the intermediate structures **C–I$_p$**, **C–I$_p$(h)** and **C–I$_p$(hp)**, NBO was carried out using the second-order perturbation theory [Equation (1)], [14].

The energy difference between donor (σ_{Nb-O}) and acceptor (σ^*_{O-H}) orbitals in the denominator decrease from **C–I$_p$(+4)** to **C–I$_p$(+5)** (8.24 and 2.65 kcal mol^{-1}, respectively). Thus, the smaller ΔE2 values are obtained for **C–I$_p$(+3)**, Table 3. The energy difference due to the Fock matrix element is small. Therefore, the magnitude of the interaction is dominated by the energy difference between the acceptor and the donor orbitals, which appears in Equation (1):

$$\Delta E2 = \frac{qF_{ij}^2}{(\varepsilon_i - \varepsilon_j)}. \quad (1)$$

From Table 3, we note that **C–I$_p$** complex is stabilized by n_{Nb}/σ^*_{O-O}, n_{Nb}/σ^*_{O-H}, $\sigma_{O-H}/\sigma^*_{O-O}$ $\sigma_{O-O}/\sigma_{O-H}^*$ and $\sigma_{Nb-O}/\sigma^*_{O-H}$ interactions, which were not present in the hexa-cluster (Figure 5). Thus the formation of the peroxo-complex **C–I$_p$(+4)** could be attributed the strong $\sigma_{Nb-O}/\sigma^*_{O-H}$ interaction (8.24 kcal mol^{-1}) (hyperconjugation between Nb–O chemical bond and hydroxyl chemical bond).

Furthermore, it was observed that **C–I$_p$(hp//+4)** is more stable than **C–I$_p$(p//+5)**, **C–I$_p$(p//+4)** and **C–I$_p$(p//+3)** by about 10.21, 15.32, and 12.65 kcal mol^{-1}, respectively. These results demonstrate that the electron attack will be preferential on the O–H chemical bond, forming a hydroperoxide molecule (Figure 6). The $\sigma_{Nb-O}/\sigma^*_{O-H}$ interaction is about 5.30 kcal mol^{-1} more effective in stabilizing the **C–I$_p$(hp//+4)** than **C–I$_p$(hp//+5)**. One of the contributions is due to the greater overlap between the O–H orbital with the Nb–O chemical bond of the catalyst.

4. Conclusion

There have been many studies aimed at developing a physical understanding of the new catalyst on the oxidation reaction. Here we highlight some basic trends encountered in the literature, the results in this paper show that niobium is a good catalyst for the

oxidation of organic dyes, and that the previous treatment of the material with hydrogen peroxide improves the catalytic activity. The better catalytic activity of the material after the previous treatment with H_2O_2 may be due to the highly reactive hydroxyl radical generated with the partial reduction of niobium.

Acknowledgements

The authors are grateful to FAPEMIG and CNPq for financial support and CBMM for samples. We would also like to thank to CENAPAD-SP for the computational facilities.

References

[1] K. Tanabe, Catal. Today **78**, 65 (2003).
[2] K. Tanabe and S.I. Okazak, Appl. Catal. A **133**, 191 (1995).
[3] E.B. Pereira, M.M. Pereira, Y.L. Lam, C.A.C. Perez, and M. Schmal, Appl. Catal. A: Gen. **197**, 99 (2000).
[4] A.L. Petre, J.A. Perdigón-Melón, A. Gervasini, and A. Auroux, Catal. Today **78**, 377 (2003).
[5] I. Nowak and M. Ziolek, Chem. Rev. **99**, 3603 (1999).
[6] M. Lu, J. Chen, and H. Huang, Chemosphere **46**, 131 (2002).
[7] R.M. Cornell and U. Schwertmann, *The Iron Oxides*, 3rd ed (Weinheim-VHC, New York, 2003).
[8] M.J. Frisch, G.W. Trucks, H.B. Schlegel, G.E. Scuseria, M.A. Robb, J.R. Cheeseman, V.G. Zakrzewski, J.A. Montgomery Jr, R.E. Stratmann, J.C. Burant, S. Dapprich, J.M. Millam, A.D. Daniels, K.N. Kudin, M.C. Strain, O. Farkas, J. Tomasi, V. Barone, M. Cossi, R. Cammi, B. Mennucci, C. Pomelli, C. Adamo, S. Clifford, J. Ochterski, G.A. Petersson, P.Y. Ayala, Q. Cui, K. Morokuma, D.K. Malick, A.D. Rabuck, K. Raghavachari, J.B. Foresman, J. Cioslowski, J.V. Ortiz, A.G. Baboul, B.B. Stefanov, G. Liu, A. Liashenko, P. Piskorz, I. Komaromi, R. Gomperts, R.L. Martin, D.J. Fox, T. Keith, M.A. Al-Laham, C.Y. Peng, A. Nanayakkara, M. Challacombe, P.M.W. Gill, B. Johnson, W. Chen, M.W. Wong, J.L. Andres, C. Gonzalez, M. Head-Gordon, E.S. Replogle, and J.A. Pople, *Gaussian 98, Revision A.9* (Gaussian, Inc, Pittsburgh PA, 1998).
[9] E.F.F. da Cunha, R.B. de Alencastro, and T.C. Ramalho, J. Theor. Comput. Chem. **3**, 1 (2004).
[10] R.R. da Silva, T.C. Ramalho, J.M. Santos, and J.D. Figueroa-Villar, J. Phys. Chem. A **110**, 1031 (2006).
[11] V. Barone, M. Cossi, and J. Tomasi, J. Comput. Chem. **19**, 404 (1984).
[12] J. Tomasi, B. Mennucci, and R. Cammi, Chem. Rev. **2105**, 2999 (2005).
[13] J.E. Carpenter and F. Weinhold, J. Mol. Struct. (Theochem) **169**, 41 (1988).
[14] E. Reed, L.A. Curtiss, and F. Weinhold, Chem. Rev. **88**, 899 (1988).
[15] D. McLean and G.S. Chandler, J. Chem. Phys. **72**, 5639 (1980).
[16] C. Gonzalez and H.B. Schlegel, J. Chem. Phys. **90**, 2154 (1989).
[17] C. Gonzalez and H.B. Schlegel, J. Phys. Chem. **94**, 5523 (1990).
[18] L.C.A. Oliveira, T.C. Ramalho, M. Gonçalves, K.T. Carvalho, and K. Sapag, Chem. Phys. Lett. **446**, 133 (2007).
[19] L.C.A. Oliveira, T.C. Ramalho, M. Gonçalves, and K. Sapag, Appl. Catal. A: Gen. **316**, 117 (2007).
[20] R. Wojcieszak, A. Jasik, S. Monteverdi, M. Ziolek, and M.M. Bettahar, J. Mol. Catal. **256**, 348 (2006).
[21] L.C.A. Oliveira, T.C. Ramalho, M. Gonçalves, and K. Sapag, Appl. Catal. B: Environ. **83**, 169 (2008).
[22] J.B. Foresman, M. Head-Gordon, J.A. Pople, and M.J. Frisch, J. Phys. Chem. **96**, 135 (1992).
[23] K. Raghavachari and G.W. Trucks, J. Chem. Phys. **91**, 1062 (1989).
[24] P. Fuentealba, H. Preuss, H. Stoll, and L. Szentpaly, Chem. Phys. Lett. **89**, 418 (1989).
[25] D. Bayot, B. Tinant, and M. Devillers, Catal. Today **78**, 439 (2003).
[26] T.C. Ramalho and C.A. Taft, J. Chem. Phys. **123**, 054319 (2005).
[27] T.C. Ramalho, T.L.C. Martins, L.E.P. Borges, and J.D. Figueroa-Villar, Int. J. Quantum Chem. **95**, 267 (2003).
[28] X. Wang, K.N. Houk, M. Spichty, and T. Wirth, J. Am. Chem. Soc. **121**, 8567 (1999).
[29] R.E. Rosenfield and R. Pathasatathy, J. Am. Chem. Soc. **99**, 4860 (1977).
[30] T. Wirth, G. Fragale, and M. Spichty, J. Am. Chem. Soc. **120**, 3376 (1998).
[31] G. Haxhillazi and H. Haeuseler, J. Solid State Chem. **177**, 3045 (2004).
[32] K.I. Selezneva and L.A. Nisel'son, Russian J. Inorg. Chem. **13**, 45 (1968).
[33] G. Boehm, Z. Krist. **63**, 319 (1926).
[34] R.N. Shchelokov, E.N. Traggeim, M.B. Varfolomeev, M.A. Michnik, and S.V. Morozova, Russian J. Inorg. Chem. **17**, 1273 (1972).
[35] D. Bayot, B. Tinant, and M. Devillers, Catal. Today **78**, 439 (2003).
[36] L.J. Burcham, J. Datka, and I.E. Wachs, J. Phys. Chem. B **103**, 6015 (1999).
[37] D. Bayot and M. Devillers, Coord. Chem. Rev. **250**, 2610 (2006).
[38] T.C. Ramalho, R.B. de Alencastro, M.A. La-Scalea, and J.D. Figueroa-Villar, Biophys. Chem. **110**, 267 (2004).
[39] U.C. Singh and P.A. Kollman, J. Comput. Chem. **5**, 129 (1984).
[40] P. Goldman, R.L. Koch, and T.C. Yeung, Biochem. Pharmacol. **35**, 43 (1986).